– –

STATE RESEARCH CENTER OF RUSSIA

INSTITUTE FOR HIGH ENERGY PHYSICS

IHEP 97-2

A.V.Berezhnoy, V.V.Kiselev, A.K.Likhoded, A.I.Onischenko

B_c MESON at LHC

Protvino 1997

UDK 539.1.01 M–24

Abstract

Berezhnoy A.V., Kiselev V.V., Likhoded A.K., Onischenko A.I. B_c MESON at LHC: IHEP Preprint 97-2. – Protvino, 1997. – p. 21, figs. 6, tables 8, refs.: 32.

In the framework of perturbative QCD and potential models of heavy quarkonium, total cross-sections and differential characteristics of hadronic production for different spin states of the B_c-meson family are calculated at energies of LHC. Theoretical predictions for masses and branching ratios of B_c decays are given, which allows one to make estimates for an expected number of reconstructed events with B_c.

Аннотация

Бережной А.В., Киселев В.В., Лиходед А.К., Онищенко А.И. B_c-мезон на LHC: Препринт ИФВЭ 97-2. – Протвино, 1997. – 21 с., 6 рис., 8 табл., библиогр.: 32.

В рамках пертурбативной КХД и потенциальных моделей тяжелого кваркония рассчитаны полные сечения и дифференциальные характеристики адронного образования различных спиновых состояний семейства B_c-мезонов при энергиях LHC. Приведены теоретические предсказания для масс и относительных вероятностей распадов B_c, что позволяет сделать оценки предполагаемого числа реконструируемых событий с B_c.

Introduction

Along with a possible direct observation of higgs particles and new particle interactions beyond the Standard Model, a detailed investigation of processes with b-quarks, involving mechanisms caused by high orders of the QCD perturbation theory, is one of the most important tasks of LHC physics program. Certainly, in the hadron decays with b-quarks the precise study of electroweak model parameters and the observation of "new" physics effects are accessible. The latter ones appear as virtual corrections to the leading approximation and, thus, must be reliably separated from the QCD high order corrections. So, the investigation of CP-violation in the heavy quark sector supposes an observation of more than 10^9 decays of B mesons. While performing this experiment it is also possible to solve another problem such as the observation of B_c meson and investigation of its properties, which are attracting a keen interest [1]. With respect to the cross-section for the production of B mesons, the yield of B_c is suppressed by a hard production of the additional heavy c-quark as well as a small probability of the $(\bar{b}c)$ state formation, so that with $\sigma(B_c^{\pm})/\sigma(b\bar{b}) \sim 10^{-3}$ one can expect about 10^6 events with B_c per 10^9 B-mesons.

The $(\bar{b}c)$ system is a mixed flavour heavy quarkonium, whose states have no annihilation decay modes due to the electromagnetic and strong interactions. Therefore, the excited levels of $(\bar{b}c)$, lying below the threshold of decay into the pair of heavy B and D mesons, follow the radiation decays into the pseudoscalar ground state, B_c^+ meson, which is a long-lived particle, decaying due to the weak interaction, $\tau(B_c) \simeq 0.55 \pm 0.15$ psec. A nonrelativistic motion of heavy quarks in the $(\bar{b}c)$ system causes a reliable application of phenomenological potential models worked out for the charmonium $(\bar{c}c)$ and bottomonium $(\bar{b}b)$, where the precision of level mass prediction reaches 30 MeV [2,3]. Weak exclusive decays of B_c are described in the framework of quark models for form-factors of different currents [4,5], which allows one also to determine the total width of this state in the form of a sum over all possible decay modes calculated. The value obtained in this way agrees with estimates of inclusive B_c decays described in the framework of the quark-hadron duality approach and operator product expansion [6]. In this consideration one takes into account the virtualities of heavy quarks in the initial state, annihilation decay channels and Pauli interference effects for the c-quark, being a product of the b-quark decay mode, with the c-quark from the initial $(\bar{b}c)$ state.

The B_c production mechanisms can be reliably investigated in the framework of perturbative QCD for a hard production of two heavy quark pairs and a potential model of a soft nonperturbative binding of $\bar{b}$ and c quarks with a small relative momentum in the system of quark mass centre. In e^+e^--annihilation at large energies ($M_{B_c}^2/s \ll 1$), the consideration of leading diagrams for the B_c-meson production gives the factorized scaling result for the differential cross-section over the energy fraction carried out by meson, $d\sigma/dz = \sigma(\bar{b}b)\cdot D(z)$, where $z = 2E_{B_c}/\sqrt{s}$ [7,8]. This distribution allows the interpretation as the hard production of heavier $\bar{b}$-quark with the subsequent fragmentation into B_c, so that $D(z)$ is the fragmentation function. In this approach one can obtain analytical expressions for the fragmentation functions into the different spin states of S, P, and D-wave levels [8]. In photon-photon interactions for the B_c production in the leading approximation of perturbation theory [9], one can isolate three gauge-invariant groups of diagrams, which can be interpreted as

1) the hard photon-photon production of $b\bar{b}$ with the subsequent fragmentation of $\bar{b} \to B_c^+(nL)$, where n is the principal quantum number of the $(\bar{b}c)$-quarkonium, $L = 0, 1\ldots$ is the orbital angular momentum;

2) the corresponding production and fragmentation for the c-quarks, and

3) the recombination diagrams of $(\bar{b}c)$-pair into B_c^+, wherein the quarks of different flavours are connected to the different photon lines.

In this case, the results of calculation for the complete set of diagrams in the leading order of perturbation theory show that the group of b-fragmentation diagrams at high transverse momenta $p_T(B_c) \gg M_{B_c}$ can be described by the fragmentation model with the fragmentation function $D_{\bar{b}\to B_c^+}(z)$, calculated in the e^+e^--annihilation. The set of c-fragmentation diagrams does not allow the description in the framework of fragmentation model. The recombination diagrams give the dominant contribution to the total cross-section for the photon-photon production of B_c.

At the LHC energies, the parton subprocess of gluon-gluon fusion $gg \to B_c^+ + b + \bar{c}$ dominates in the hadron-hadron production of B_c mesons. In the leading approximation of QCD perturbation theory it requires the calculation of 36 diagrams in the fourth order over the α_s coupling constant. In this case, there are no isolated gauge-invariant groups of diagrams, which would allow the interpretation similar to the consideration of B_c production in e^+e^--annihilation and photon-photon collisions.

The calculation for the complete set of diagrams of the $O(\alpha_s^4)$-contribution allows one to determine a value of the transverse momentum p_T^{min}, being the low boundary of the region, where the subprocess of gluon-gluon B_c-meson production enters the regime of factorization for the hard production $b\bar{b}$-pair and the subsequent fragmentation of $\bar{b}$-quark into the bound $(\bar{b}c)$-state, as it follows from the theorem on the factorization of the hard processes in the perturbative QCD [10].

The p_T^{min} value turns out to be much greater than the M_{B_c} mass, so that the dominant contribution into the total cross-section of gluon-gluon B_c-production is given by the diagrams of nonfragmentational type, i.e. by the recombination of heavy quarks. Furthermore, the convolution of the parton cross-section with the gluon distributions inside the initial hadrons leads to the suppression of contributions at large transverse momenta as well as the subprocesses with large energy in the system of parton mass centre, so that the main contribution into the total cross-section of hadronic B_c-production is given by the region of energies less or comparable to the B_c-meson mass, where the fragmentation model can not be applied by its construction. Therefore, one must perform the calculations with account for all contributions to the order under consideration in the region near the threshold.

In this work we calculate both the total and differential cross-sections for the production of S- and P-wave states of B_c mesons in the framework of leading order of the QCD perturbation theory. Below we give quite a complete set of the B_c characteristics. The basic spectroscopic characteristics of the $(\bar{b}c)$ family and the branching ratios of different decay modes of the pseudoscalar ground state, which can be used for the extraction of the B_c signal from the hadronic background, are presented in Section 1. The calculations of characteristics in the hadronic B_c production are analyzed in Section 2. In Conclusion the obtained results are summarized.

1. The spectroscopy and decays of B_c

1.1. Level masses and coupling constants

As a system containing two heavy quarks, the $(\bar{b}c)$-mesons can be reliably described in the framework of phenomenological nonrelativistic potential models [11] and in QCD sum rules [12], which are based on (i) the formalism of the expansion over the inverse heavy quarks mass, due to a small ratio of the typical quark virtualities, being of the order of the confinement scale, to the mass, and (ii) the expansion over a small relative velocity of the quark motion in the bound state. The perturbative QCD allows one to take into account hard gluon corrections to the currents of effective quarks, defining the leading approximation in these expansions [13]. This way of consideration leads to quite a precise and reliable description of the families of $(\bar{c}c)$-charmonium and $(\bar{b}b)$-bottomonium, whose spectroscopic properties are in detail studied experimentally [14].

The effective gluon potential of static quarks does not depend on the flavour of a heavy quark. The different phenomenological models lead to the potential, whose form in the range of average distances between the quarks for ground and excited levels:$0.1 < r < 1$ fm, really does not depend on the model [15]. The experimental data on the $(\bar{c}c)$ and $(\bar{b}b)$ systems point out the energy level regularity expressed in the approximate quark-flavour independence of the difference between energies of excitations. According to the Hell-Mann – Feynman theorem, this regularity is caused by the constant value of average kinetic energy of the heavy quarks. This energy does not depend on the quark flavours and the number of excitation. The independence becomes exact for the logarithmic potential [16]. The weak dependence of the difference between energy levels can be taken into account while considering Martin potential: $V(r) = A(r/r_0)^a + C$ [17].

The mass values for the different states of $(\bar{b}c)$ system in the Martin potential with account for the spin-dependent splitting of nL-levels are presented in Table 1 in comparison with the estimates performed in the BT-potential, which is motivated by QCD with the account for the two-loop evolution of the coupling constant at short distances [19]. The spectroscopic notations of states are $n^{2j_c}L_J$, where j_c is the total angular momentum of c-quark, n is the principal quantum number, L is the orbital angular momentum, J is the total spin of meson. The splittings are calculated in the second order of $1/m_Q$-expansion over the inverse heavy quark mass with account for the vector coupling of the effective one-gluon exchange between the quarks and scalar coupling for the part of potential confining the quarks in the bound state [18]. The effective value of the gluon coupling constant at the scale of the average momentum transfer between the quarks can be determined over the known experimental value for the splitting of charmonium $1S$-level with the taking into account the renormalization group evolution towards the $(\bar{b}c)$ energies [2].

Table 1. The masses of bound $(\bar{b}c)$-states below the threshold of decay into the pair of heavy mesons BD, in GeV.

state	Martin[2]	BT[3]
1^1S_0	6.253	6.264
1^1S_1	6.317	6.337
2^1S_0	6.867	6.856
2^1S_1	6.902	6.899
2^1P_0	6.683	6.700
$2P\ 1^+$	6.717	6.730
$2P\ 1'^+$	6.729	6.736
2^3P_2	6.743	6.747
3^1P_0	7.088	7.108
$3P\ 1^+$	7.113	7.135
$3P\ 1'^+$	7.124	7.142
3^3P_2	7.134	7.153
$3D\ 2^-$	7.001	7.009
3^5D_3	7.007	7.005
3^3D_1	7.008	7.012
$3D\ 2'^-$	7.016	7.012

Thus, in the $(\bar{b}c)$ system below the threshold of decay into the heavy meson BD pair, one can expect the presence of 16 narrow states of the $1S$, $2S$,$2P$, $3P$ and $3D$-levels, which cascadely transform into the ground pseudoscalar state with the mass $m_{B_c} = 6.25 \pm 0.03$ GeV due to the emission of photons and π-meson pairs, since the annihilation $(\bar{b}c)$ decays can occur only due to the weak interaction and, hence, are suppressed for the excited levels. The total widths of the excited states and the branching ratios for the radiation modes of decay are shown in Table 2.

Table 2. The total widths of excited bound $(\bar{b}c)$-states below the threshold of decay into the meson BD-pair in the model with Martin potential and the branching ratios of the dominant decay modes.

state	$\Gamma_{\rm tot}$, KeV	dominant decay mode	BR, %
1^1S_1	0.06	$1^1S_0+\gamma$	100
2^1S_0	67.8	$1^1S_0+\pi\pi$	74
2^1S_1	86.3	$1^1S_1+\pi\pi$	58
2^1P_0	65.3	$1^1S_1+\gamma$	100
$2P\ 1^+$	89.4	$1^1S_1+\gamma$	87
$2P\ 1'^+$	139.2	$1^1S_0+\gamma$	94
2^3P_2	102.9	$1^1S_1+\gamma$	100
3^1P_0	44.8	$2^1S_1+\gamma$	57
$3P\ 1^+$	65.3	$2^1S_1+\gamma$	49
$3P\ 1'^+$	92.8	$2^1S_0+\gamma$	63
3^3P_2	71.6	$2^1S_1+\gamma$	69
$3D\ 2^-$	95.0	$2P\ 1^++\gamma$	47
3^5D_3	107.9	$2^3P_2+\gamma$	71
3^3D_1	155.4	$2^1P_0+\gamma$	51
$3D\ 2'^-$	122.0	$2P\ 1'^++\gamma$	38

The potentials motivated by QCD have the linear growth at large distances and the coulumb-like behaviour at short ones. The form of the potential in the region, where the perturbative regime changes into the nonperturbative one with the increase of the distance between the quarks, coincides with the form of the logarithmic or power potentials, so that the accuracy for the prediction of the energy levels in the heavy quarkonia, particular in the $(\bar{b}c)$ system, is determined by the value of 30 MeV.

The global properties of these potentials, i.e. their asymptotic behaviour in the bound points of $r\to\infty$, $r\to 0$, are significant for the determination of the coupling constants of the states, such as, e.g., the leptonic coupling constants f for the nS-levels. In the leading approximation, the f value does not depend on the spin state of the level and it is determined by the value of the radial wave function at the origin, $R(0)$,

$$\tilde{f}_n=\sqrt{\frac{3}{\pi M_n}}R_{nS}(0)\ .$$

Taking into account the hard gluon corrections [20,21], the constants of vector and pseudoscalar states equal

$$f_n^{V,P}=\tilde{f}_n\left(1+\frac{\alpha_s}{\pi}\left(\frac{m_1-m_2}{m_1+m_2}\ln\frac{m_1}{m_2}-\delta^{V,P}\right)\right)\ , \tag{1}$$

where $m_{1,2}$ are the quark masses, $\delta^V=8/3$, $\delta^P=2$, and the QCD coupling constant is determined at the scale of the gluon virtuality, given by the quark masses function [22].

The values of the heavy quarkonium wave functions are significant in the consideration of production and decays of their states in the framework of quark models of the mesons. They are shown in Table 3 for S- and P-wave states in the model with the Martin potential. However, as it was mentioned above, the accuracy of potential models for the values under consideration is quite low, and the uncertainty is expressed by a factor of two.

Table 3. The wave function characteristics, $R_{nS}(0)$ (in GeV$^{3/2}$) and $R'_{nP}(0)$ (in GeV$^{5/2}$), obtained from the Schrödinger equation with the Martin potential and BT.

n	Martin[2]	BT[3]
$R_{1S}(0)$	1.31	1.28
$R_{2S}(0)$	0.97	0.99
$R'_{2P}(0)$	0.55	0.45
$R'_{3P}(0)$	0.57	0.51

The QCD sum rules allow one to determine the leptonic constants for the heavy quarkonium states with a much better accuracy. Standard schemes of the sum rules give an opportunity to calculate the ground state constants for vector and pseudoscalar currents with account for corrections from the quark-gluon condensates, which have the power form over the inverse heavy quark mass [12]. There is a region of the momentum numbers for the spectral density of the two-point current correlator, where the condensate contributions are not significant. In this region, the integral representation for the contribution of resonances lying below the threshold of decay into the pair of heavy mesons, allows one to use the regularity of the quarkonium state density mentioned above, and to derive the scaling relations for the leptonic constants of the ground state quarkonia with different quark contents and for the excited states [21]. Thus, for vector states we have

$$\frac{f_n^2}{M_n}\left(\frac{M_n}{M_1}\right)^2\left(\frac{m_1+m_2}{4m_{12}}\right)^2=\frac{c}{n}\,, \tag{2}$$

where $m_{12} = m_1m_2/(m_1 + m_2)$ is the reduced mass of quarks, and the constant c is determined by the average kinetic energy of quarks, the QCD coupling constant at the scale of average momentum transfers in the system and the hard gluon correction factor to the vector current. Numerically, the c value does not turn out to be dependent on any quark flavour and excitation number in the system. Relation (2) is in a good agreement with the data on the coupling constants for the families of ψ and Υ particles and, thus, it can be a reliable basis for the prediction of leptonic constants for the B_c-meson family, as it is shown in Table 4, where one can also find the constants for the pseudoscalar states of nS-levels, which are determined by relation (see [21])

$$f_n^P = f_n\left(1+\frac{2\alpha_s}{3\pi}\right)\frac{m_1+m_2}{M_n}\,.$$

The $R(0)$ values, being the parameters of static quark models in the consideration of decays and production of the mesons, can be determined over the leptonic constants calculated in the sum rules. In this way, the additional uncertainty appears. It is related to a choice of the scale fixing the QCD coupling constant in the factor accounting for the hard gluon correction. The dependence on this choice points out the significance of high orders in the perturbative approximation. Assuming that in the $\overline{\rm MS}$-scheme the scale is close to $\mu^2 = m_1 m_2 e^{-11/12}$ [22], one obtains the values of $R(0)$ shown in Table 4, where one can see that the predictions of sum rules and the potential models of Martin and BT are in a reasonable agreement with each other.

Table 4. The leptonic constants for the vector and pseudoscalar states of nS-levels in the $(\bar{b}c)$-system, f_n and f_n^P, calculated in the sum rules resulting in the scaling relation, and $R_{nS}(0)$, calculated over f_n. The accuracy is equal to 6%.

n	f_n, MeV	f_n^P, MeV	$R_{nS}(0)$, GeV$^{3/2}$
1	385	397	1.20
2	260	245	0.85

As for the states lying above the threshold of decay into the heavy meson BD pair, the width of $B_c^{*+}(3S) \to B^+ D^0$, for example, can be calculated in the framework of sum rules for the meson currents, where the scaling relation takes place for the g constants of similar decays of $\Upsilon(4S) \to B^+ B^-$ and $\psi(3770) \to D^+ D^-$ [23],

$$\frac{g^2}{M}\left(\frac{4m_{12}}{M}\right) = const.$$

The relation is caused by the dependence of energy gap between the vector and pseudoscalar heavy meson states: $\Delta M_{1,2} \cdot M_{1,2} = const.$, where $M_{1,2}$ are the meson masses in the final state, m_{12} is their reduced mass. The width of this decay has a strong dependence on the $B_c^{*+}(3S)$ mass, and at $M = 7.25$ GeV it is equal to $\Gamma = 90 \pm 35$ MeV, where the uncertainty is determined by the accuracy of the method used.

1.2. The B_c meson decays

1.2.1. Life-time

The B_c-meson decay processes can be subdivided into three classes: 1) the $\bar{b}$-quark decay with the spectator c-quark, 2) the c-quark decay with the spectator $\bar{b}$-quark and 3) the annihilation channel $B_c^+ \to l^+ \nu_l (c\bar{s}, u\bar{s})$, where $l = e,\ \mu,\ \tau$. In the $\bar{b} \to \bar{c}c\bar{s}$ decays one separates also the Pauli interference with the c-quark from the initial state. In accordance with the given classification, the total width is the sum over the partial widths

$$\Gamma(B_c \to X) = \Gamma(b \to X) + \Gamma(c \to X) + \Gamma(\text{ann.}) + \Gamma(\text{PI})\ . \tag{3}$$

For the annihilation channel the $\Gamma(\text{ann.})$ width can be reliably estimated in the framework of inclusive approach, where one takes the sum of the leptonic and quark decay modes with account for the hard gluon corrections to the effective four-quark interaction of weak currents. These corrections result in the factor of $a_1 = 1.22 \pm 0.04$ [1]. The width is expressed through the leptonic constant of $f_{B_c} = f_1^P \approx 400$ MeV. This estimate of the quark-contribution does not depend on a hadronization model, since the large energy release of the order of the meson mass takes place. As is seen from the following expression, one can neglect the contribution by light leptons and quarks

$$\Gamma(\text{ann.}) = \sum_{i=\tau,c} \frac{G_F^2}{8\pi}|V_{bc}|^2 f_{B_c}^2 M m_i^2 (1 - m_i^2/m_{Bc}^2)^2 \cdot C_i \,, \tag{4}$$

where $C_\tau = 1$ for the $\tau^+\nu_\tau$-channel and $C_c = 3|V_{cs}|^2 a_1^2$ for the $c\bar{s}$-channel.

As for the nonannihilation decays, in the approach of the operator product expansion for the quark currents of weak decays [6], one takes into account the α_s-corrections to the free quark decays and uses the quark-hadron duality for the final states. Then one considers the matrix element for the transition operator over the bound meson state. The latter also allows one to take into account effects caused by the motion and virtuality of decaying quark inside the meson because of the interaction with the spectator. In this way the $\bar{b} \to \bar{c}c\bar{s}$ decay mode turns out to be suppressed almost completely due to the Pauli interference with the charm quark from the initial state. Besides, the c-quark decays with the spectator $\bar{b}$-quark are essentially suppressed in comparison with the free quark decays because of a large bound energy in the initial state.

In the framework of exclusive approach it is necessary to sum widths of different decay modes calculated in the potential models [4,5]. While considering the semileptonic decays due to the $\bar{b} \to \bar{c}l^+\nu_l$ and $c \to sl^+\nu_l$ transitions one finds that in the former decays the hadronic final state is practically saturated by the lightest bound $1S$-state in the $(\bar{c}c)$-system, i.e. by the η_c and J/ψ particles, and in the latter decays the $1S$-states in the $(\bar{b}s)$-system, i.e. B_s and B_s^*, only can enter the accessible energetic gap. The energy release in the latter transition is low in comparison with the meson masses, and, therefore, a visible deviation from the picture of quark-hadron duality is possible. Numerical estimates show that the value of $B_c \to (\bar{b}s)l^+\nu_l$ decay width is two times less in the exclusive approach than in the inclusive method, though this fact can be caused by the choice of narrow wave package for the $B_s^{(*)}$ mesons in the quark model, so that $\tilde{f}_{B_s} \approx 150$ MeV, while in the limit of static heavy quark, one should expect a larger value for the leptonic constant [24,25]. This increase will lead to the widening of the wave package and, hence, to the increase of the overlapping integral for the wave functions of B_c and $B_s^{(*)}$ (see table 5).

Further, the $\bar{b} \to \bar{c}u\bar{d}$ channel, for example, can be calculated through the given decay width of $\bar{b} \to \bar{c}l^+\nu_l$ with account for the color factor and hard gluon corrections to the four-quark interaction. It can be also obtained as a sum over the widths of decays with the $(u\bar{d})$-system bound states.

The results of calculation for the total B_c width in the inclusive and exclusive approaches give the values consistent with each other, if one takes into account the most significant uncertainty related with the choice of quark masses (especially for the charm quark), so that finally we have

$$\tau(B_c^+) = 0.55 \pm 0.15 \text{ psec.} \tag{5}$$

Table 5. The branching ratios of the B_c decay modes calculated in the framework of inclusive approach and in the exclusive quark model with the parameters $|V_{bc}| = 0.040$, $\tilde{f}_{B_c} = 0.47$ GeV, $\tilde{f}_\psi = 0.54$ GeV,$\tilde{f}_{B_s} = 0.3$ GeV, $m_b = 4.8 - 4.9$ GeV, $m_c = 1.5 - 1.6$ GeV, $m_s = 0.55$ GeV. The accuracy is about 10%.

B_c decay mode	Inclus., %	Exclus., %
$\bar{b} \to \bar{c}l^+\nu_l$	3.9	3.7
$\bar{b} \to \bar{c}u\bar{d}$	16.2	16.7
$\sum \bar{b} \to \bar{c}$	25.0	25.0
$c \to sl^+\nu_l$	8.5	10.1
$c \to su\bar{d}$	47.3	45.4
$\sum c \to s$	64.3	65.6
$B_c^+ \to \tau^+\nu_\tau$	2.9	2.0
$B_c^+ \to c\bar{s}$	7.2	7.2

1.2.2. Exclusive decays

The consideration of exclusive B_c-decay modes supposes an introduction of model for the hadronization of quarks into the mesons with the given quantum numbers. The QCD sum rules for the three-point correlators of quark currents [26,27] and potential models [4,5] are among those hadronization models. A feature of the sum rule application to the mesons containing two heavy quarks, is the account for the significant role of the coulumb-like α_s/v-corrections due to the gluon exchange between the quarks composing the meson and moving with the relative velocity v. So, in the semileptonic decays of $B_c^+ \to \psi(\eta_c)l^+\nu_l$, the heavy $(\bar{Q}_1 Q_2)$ quarkonium is present in both the initial and final states, and, therefore, the contribution of coulumb-like corrections exhibits itself in a particulary strong form. The use of tree approximation for the perturbative contribution into the three-point correlator of quark currents [26] leads to a large deviation between the values of transition form-factors, calculated in the sum rules and potential models, respectively. The account for the α_s/v-corrections removes this contradiction [27]. Thus, the meson potential models, based on the covariant expression for the form-factors of weak B_c decays through the overlapping of quarkonium wave functions in the initial and final states, and the QCD sum rules give the consistent description of semileptonic B_c-meson decays.

Further, the hadronic decay widths can be obtained on the basis of assumption on the weak transition factorization between the quarkonia and the hadronization of products of the virtual W^{*+}-boson decay [28]. The accuracy of factorization has to rise with the increase of W-boson virtuality. This fact is caused by the suppression of interaction in the final state. In this way, the hadronic decays can be calculated due to the use of form-factors for the semileptonic transitions with the relevant description of W^* transition into the hadronic state.

Let us consider the amplitude of $B_c^+ \to M_X e^+ \nu_e$ transition with the weak decay of quark 1 into quark 2

$$A = \frac{G_F}{\sqrt{2}} V_{12}\, l_\mu\, H^\mu\ , \tag{6}$$

where G_F is the Fermi constant, V_{12} is the Kobayashi-Maskawa matrix element. The leptonic l_μ current is determined by the expression

$$l_\mu = \bar{e}(q_1)\gamma_\mu(1-\gamma_5)\nu(q_2)\ , \tag{7}$$

where $q_{1,2}$ are the momenta of lepton and neutrino, correspondingly; $(q_1+q_2)^2 = t$. The H_μ value in (6) is the matrix element for the hadronic J_μ current

$$J_\mu = V_\mu - A_\mu = \bar{Q}_1\gamma_\mu(1-\gamma_5)Q_2\ . \tag{8}$$

The matrix element for the B_c decay into the pseudoscalar P state can be written down in the form

$$< B_c(p)|A_\mu|P(k) >= F_+(t)(p+k)_\mu + F_-(t)(p-k)_\mu\ , \tag{9}$$

and for the transition into the vector V meson with the M_V mass and λ polarization one can express the matrix element in the form

$$\begin{aligned} < B_c(p)|\quad J_\mu\quad |V(k,\lambda) >= & -(M+M_V)A_1(t)\, \epsilon_\mu^{(\lambda)} + \frac{A_2(t)}{M+M_V}\, (\epsilon^{(\lambda)}p)\ (p+k)_\mu \\ & + \frac{A_3(t)}{M+M_V}\, (\epsilon^{(\lambda)}p)\ (p-k)_\mu + i\frac{2V(t)}{M+M_V}\ \epsilon_{\mu\nu\alpha\beta}\ \epsilon^{(\lambda)\nu}p^\alpha k^\beta. \end{aligned} \tag{10}$$

Relations (9), (10) define the form-factors for the $B_c^+ \to M_X e^+ \nu_e$ transitions, so that for the massless leptons, F_- and A_3 do not contribute into the matrix element in (6). In the covariant quarkonium model with the wave functions of oscillator type [4] one can easily obtain

$$F_+(t) \ = \ \frac{1}{2}\,(m_1+m_2)\sqrt{\frac{M_P}{M}}\frac{1}{m_2}\xi_P(t)\ , \tag{11}$$

$$F_-(t) \ = \ -\frac{1}{2}\,(m_1-m_2+2m_{sp})\sqrt{\frac{M_P}{M}}\frac{1}{m_2}\xi_P(t)\ , \tag{12}$$

where m_{sp} is the mass of spectator quark, and the $\xi(t)$ function has the form

$$\xi_X(t) = \frac{2\omega\omega_X}{\omega^2+\omega_X^2}\sqrt{\frac{2\omega\omega_X}{\omega^2y^2+\omega_X^2}}\exp\Big\{-\frac{m_{sp}^2}{\omega^2y^2+\omega_X^2}\,(y^2-1)\Big\}\ , \tag{13}$$

where M_X is the meson mass, and ω_X is the wave function parameter of the recoil meson,

$$y = 1+\frac{t_m-t}{2MM_X},\quad t_m = (M-M_X)^2,\quad \tilde{f}_X = \sqrt{\frac{12}{M_X}\Big(\frac{\omega_X^3}{2\pi}\Big)^{3/2}}\ , \tag{14}$$

t_m is the maximum square of the leptonic pair mass. For the vector state $M_V = M_X$ we get

$$V(t) = \frac{1}{2}\,(M+M_V)\sqrt{\frac{M_V}{M}}\frac{1}{m_2}\xi_V(t)\;, \tag{15}$$

$$A_1(t) = \frac{1}{2}\,\frac{M^2+M_V^2-t+2M(m_2-m_{sp})}{M+M_V}\sqrt{\frac{M_V}{M}}\frac{1}{m_2}\xi_V(t)\;, \tag{16}$$

$$A_2(t) = \frac{1}{2}\,(M+M_V)(1-2m_{sp}/M)\sqrt{\frac{M_V}{M}}\frac{1}{m_2}\xi_V(t)\;, \tag{17}$$

$$A_3(t) = -\frac{1}{2}\,(M+M_V)(1+2m_{sp}/M)\sqrt{\frac{M_V}{M}}\frac{1}{m_2}\xi_V(t)\;. \tag{18}$$

The branching ratios of some exclusive B_c-decay modes are shown in Table 6.

Table 6. The branching ratios of exclusive B_c decay modes, calculated in the framework of covariant quark model with the parameters $|V_{bc}| = 0.040$, $\tilde{f}_{B_c} = 0.47$ GeV, $\tilde{f}_\psi = 0.54$ GeV, $\tilde{f}_{B_s} = 0.3$ GeV, $m_b = 4.8-4.9$ GeV, $m_c = 1.5-1.6$ GeV, $m_s = 0.55$ GeV. The accuracy equals 10%.

B_c decay mode	BR, %	B_c decay mode	BR, %
$\psi l^+\nu_l$	2.5	$\eta_c l^+\nu_l$	1.2
$B_s^* l^+\nu_l$	6.2	$B_s l^+\nu_l$	3.9
$\psi\pi^+$	0.2	$\eta_c\pi^+$	0.2
$B_s^*\pi^+$	5.2	$B_s\pi^+$	5.5
$\psi\rho^+$	0.6	$\eta_c\rho^+$	0.5
$B_s^*\rho^+$	22.9	$B_s\rho^+$	11.8

A decrease of the invariant mass for the hadron system results in an increase of the recoil meson momentum. This causes the problem of applicability for the formalism of overlapping for the quarkonium wave functions, because, in this kinematics, the narrow wave packages are displaced relative to each other in the momentum space into the range of distribution tails. In this situation one has to take into account a hard gluon exchange between the quarkonium constituents, which destroys the spectator picture of weak transition in the potential approach. For example, the widths of $B_c^+ \to \psi\pi^+$ and $B_c^+ \to \eta_c\pi^+$ decays have the following forms [29]

$$\Gamma(B_c^+\to\psi\pi^+) = G_F^2|V_{bc}|^2\,\frac{128\pi\alpha_s^2}{81}f_\pi^2\tilde{f}_{B_c}^2\tilde{f}_\psi^2\left(\frac{M+m_\psi}{M-m_\psi}\right)^3\frac{M^3}{(M-m_\psi)^2m_\psi^2}\,a_1^2, \tag{19}$$

$$\frac{\Gamma(B_c^+\to\eta_c\pi^+)}{\Gamma(B_c^+\to\psi\pi^+)} = \frac{(5(M-m_{\eta_c})(M^2-m_{\eta_c}^2)+(M-m_{\eta_c})^3+8m_{\eta_c}^3)^2}{16(M+m_{\eta_c})^2M^4}\,. \tag{20}$$

As one can see from equations (19)-(20), the basic uncertainty in the width estimation is connected with the scale choice for the "running" QCD coupling constant, which supposes the renormalization of the six-quark operator for the transition between the quarkonia in the next-to-tree approximation. This problem requires carrying out a large volume of cumbersome calculations. However, even at this stage of evaluations one can state that the corrections with "large" logarithms are expected to appear from the contributions related to the renormalization of four-quark weak interaction (the a_1 factor) and in the gluon propagator standing in the exchange between the quarks. The latter leads to the fixing of α_s scale at the gluon virtuality. Numerically, this virtuality is determined by the recoil meson momentum, and it is slightly greater than 1 GeV, so that one can speak on a quite hard gluon exchange, which gives the values of branching ratios of approximately one order of magnitude greater than in the potential approach, as one can find in Table 7. However, the conservative estimate of uncertainty in the hard approximation is close to 50%.

Table 7. The branching ratios of exclusive B_c decay modes at the large momenta of recoil meson in the framework of hard gluon exchange approximation. The uncertainty equals 50%.

B_c decay mode	BR., %	B_c decay mode	BR, %
$\psi\pi^+$	2.0	$\eta_c\pi^+$	2.6
$\psi\rho^+$	5.6	$\eta_c\rho^+$	7.2

As for the extraction of B_c signal in the hadronic background, the decay modes with ψ in the final state are the most preferable, because the latter particle can be easily identified by its leptonic decay mode. This advantage is absent in the B_c decay modes with the final state containing the η_c or $B_s^{(*)}$ mesons, which are the objects, whose experimental detection is impeded by a large hadron background. From the values of branching ratios shown above one can easily find, that the total probability of ψ yield in the B_c decays equals $\mathrm{BR}(B_c^+ \to \psi X) = 0.24$. It is worth noting that the key role in the B_c signal observation plays the presence of the vertex detector, which allows one to extract events with the weak decays of long-lived particles containing heavy quarks. In the case under consideration it gives the possibility to suppress the background from the direct ψ production. In the semileptonic $B_c^+ \to \psi l^+\nu_l$ decays the presence of vertex detector and large statistics of events allows one to determine the B_c-meson mass and separate the events with its decays from the ordinary B_u^+-meson decays, which have no ψl^+ mode. In the $\psi\pi^+$ decay the direct measurement of B_c mass is possible. The detector efficiency in the reconstruction of three-particle secondary vertex (l^+l^- from decays of ψ and π^+ or l^+) becomes the most important characteristics here. The low efficiency of the LEP detectors ($\epsilon \approx 0.15$), for example, makes the B_c observation to be probably unachivable in the experiments at the electron-positron collider [30].

2. The characteristics of B_c production at LHC

As was mentioned above, the consideration of mechanisms for the hadronic production of different spin B_c-states is based on the factorization of hard parton production of heavy quarks ($\bar{b}b\bar{c}c$) and soft coupling of ($\bar{b}c$) bound state [10]. At the first stage of description, the hard subprocess can be reliably calculated in the framework of QCD perturbation theory, while in the second stage the quark binding in the heavy quarkonium can be described in the nonrelativistic potential model assigned to the ($\bar{b}c$)-pair rest system. The latter means that one performs the integration of the final quark state over the quarkonium wave function in the momentum space. Since the relative quark velocity inside the meson is close to zero, the perturbative matrix element can be expanded in series over the relative quark momentum, which is low in comparison with the quark masses determining the scale of virtualities and energies in the matrix element. In the leading approximation one considers only the first nonzero term of such expansion, so that for the S-wave states the matrix element of the parton subprocess for the B_c production is expressed through the perturbative matrix element for the production of four heavy quarks ($gg \to \bar{b}b\bar{c}c$) with the corresponding projection to the vector or pseudoscalar spin state of ($\bar{b}c$)-system, being the color singlet, and through the factor of radial wave function at the origin, $R_{nS}(0)$, for the given quarkonium. The perturbative matrix element is calculated for the ($\bar{b}c$) state, where the quarks move with the same velocity, i.e. one neglects the relative motion of $\bar{b}$ and c.

For the P-wave states, the potential model gives the factor in the form of the first derivative of the radial wave function at the origin, $R'_{nL}(0)$. In the perturbative part, one has to calculate the first derivative of the matrix element over the relative quark momentum at the point, where the velocities of quarks, entering the quarkonium, equal each other.

Thus, in addition to the heavy quark masses, the values of $R_{nS}(0)$, $R'_{nL}(0)$ and α_s are the parameters of calculation for the partonic production of B_c meson. In calculations we use the wave function parameters equal to the values shown in Table 4 and $R'_{2P}(0) = 0.50$ GeV$^{3/2}$. The value of $R(0)$, as was shown above, can be related with the leptonic constant, $\tilde{f}$, so that we have

$$\tilde{f}_{1S} = 0.47 \text{ GeV}, \quad \tilde{f}_{2S} = 0.32 \text{ GeV}.$$

At large transverse momenta of the B_c meson, $p_T \gg M_{B_c}$, the production mechanism enters the regime of $\bar{b}$-quark fragmentation (see Fig. 1), so that the scale determining the QCD coupling constant in hard $\bar{b}b$ production, is given by $\mu^2_{\bar{b}b} \sim M^2_{B_c} + p^2_T$, and in the hard fragmentation production of the additional pair of heavy quarks $\bar{c}c$ we get $\mu_{\bar{c}c} \sim m_c$. This scale choice is caused by the high order corrections of perturbation theory to the hard gluon propagators, where the summing of logarithms over the virtualities leads to the pointed μ values. Therefore, the normalization of matrix element is determined by the value of $\alpha_s(\mu_{\bar{b}b})\alpha_s(\mu_{\bar{c}c}) \approx 0.18 \cdot 0.28$. In calculations we use the single combined value of $\alpha_s = 0.22$.

In the approximation of the weak quark binding inside the meson, one has $M_{B_c} = m_b + m_c$, so that the performable phase space in calculations is close to physical one at the choices of $m_b = 4.8$ GeV, $m_c = 1.5$ GeV for the $1S$-state, $m_b = 5.1$ GeV, $m_c = 1.8$ GeV for the $2S$-state, $m_b = 5.0$ GeV, $m_c = 1.7$ GeV for the $2P$-state. The value of the hadron-hadron cross-section is determined by the convolution of parton distributions with the cross-sections of parton subprocesses. At the LHC energies the subprocess of $gg \to B_c^+ b\bar{c}$ is dominant in the production of B_c meson because of the more high gluon-gluon luminosity. The total cross-sections of the subprocesses for different spin states of B_c meson are calculated numerically, and their dependence on the subprocess energy, $\sqrt{\hat{s}}$, can be written down in the following analytic approximation

$$\sigma(gg \to B_c(1S)\, b\bar{c}) = 550.0 \left(1 - \frac{2(m_b + m_c)}{\sqrt{\hat{s}}}\right)^{2.35} \cdot \left(\frac{2(m_b + m_c)}{\sqrt{\hat{s}}}\right)^{1.37} \text{pb}, \quad (21)$$

$$\sigma(gg \to B_c(2P)\, b\bar{c}) = 25.0 \left(1 - \frac{2(m_b + m_c)}{\sqrt{\hat{s}}}\right)^{1.95} \cdot \left(\frac{2(m_b + m_c)}{\sqrt{\hat{s}}}\right)^{1.2} \text{pb}, \quad (22)$$

in the region of $2(m_b + m_c) < \sqrt{\hat{s}} < 400$ GeV.

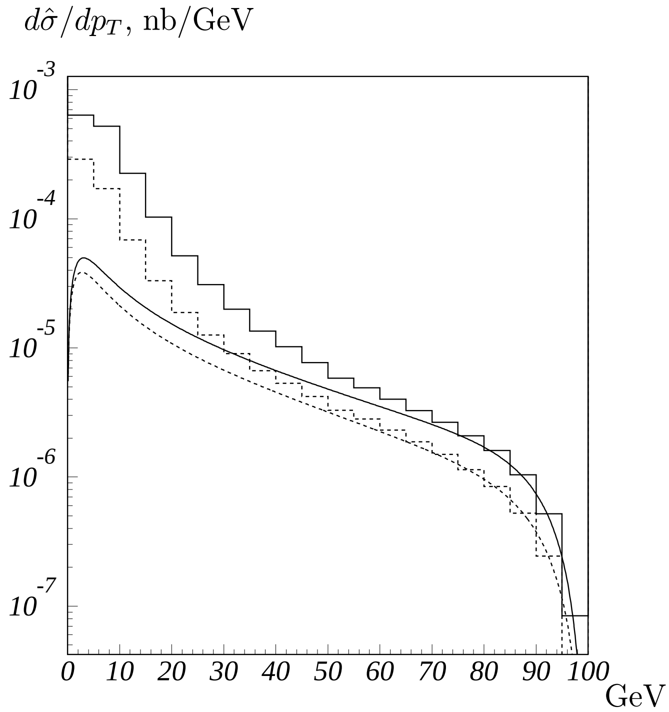

Fig. 1. The differential cross-section for the $B_c^{(*)}$ meson production in gluon-gluon collisions as calculated in the perturbative QCD over the complete set of diagrams in the $O(\alpha_s^4)$ order at 200 GeV. The dashed and solid histograms present the pseudoscalar and vector states, respectively, in comparison with the results of fragmentation model shown by the corresponding smooth curves.

The using of CTEQ4M parameterization for the structure functions of nucleon [31] leads to the total hadronic cross-sections for the B_c mesons, as shown in Table 8. After the summing over the different spin states, the total cross-sections for the production of P-wave levels is equal to 7% of the S-state cross-section.

Table 8. The total cross-sections for the hadronic production of different spin states of the B_c mesons at the LHC energies.

nL_J	σ(8 TeV), nb	σ(16 TeV), nb
$1S_0$	21.961	46.104
$1S_1$	55.039	115.493
$2S_0$	4.818	10.115
$2S_1$	12.022	25.226

In Fig. 2 the $d\sigma/dp_T$ distributions over the transverse momentum for the yields of $1S$-states of B_c and B_c^* are shown at the 8 and 16 TeV energies. The maximum in the distribution is reached at $p_T \sim M_{B_c}$. From the distribution over rapidity (Fig. 3) one can see that the production of B_c meson takes place basically in the central region. The topology of events with the B_c-meson production somewhat differs from the configuration for the B meson. In the system of mass centre for the final $B_c + b + \bar{c}$ state, the B_c and b particles mainly move in opposite directions. Otherwise, as it is shown in Fig. 4, the $\bar{c}$-quark moves in the same direction as the B_c meson. The distribution over the angle between the B_c meson and $\bar{c}$-quark has the sharp maximum in the region of $0.95 < \cos\theta < 1$.

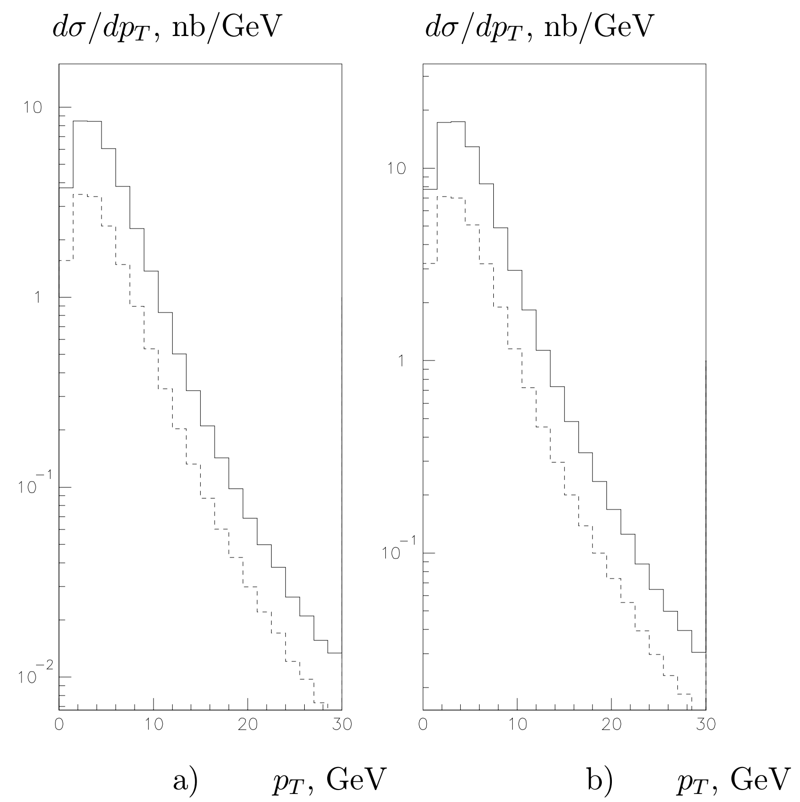

Fig. 2. The distributions over the transverse momentum of B_c^* (solid line) and B_c (dashed line) in proton-proton interactions at the energies of 8 TeV (a) and 16 TeV (b).

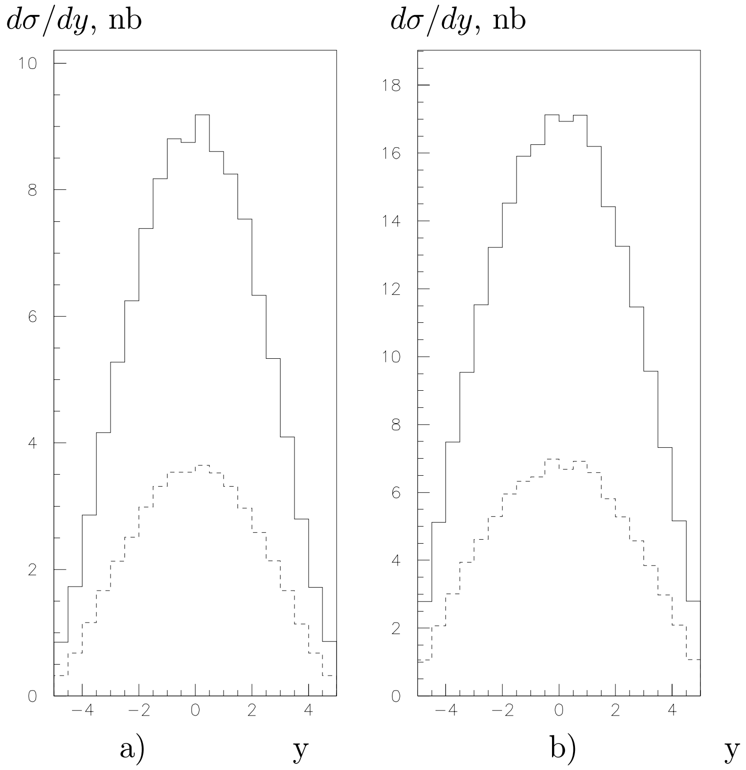

Fig. 3. The distributions over the rapidities of B_c^* (solid line) and B_c (dashed line) in proton-proton interactions at the energies of 8 TeV (a) and 16 TeV (b).

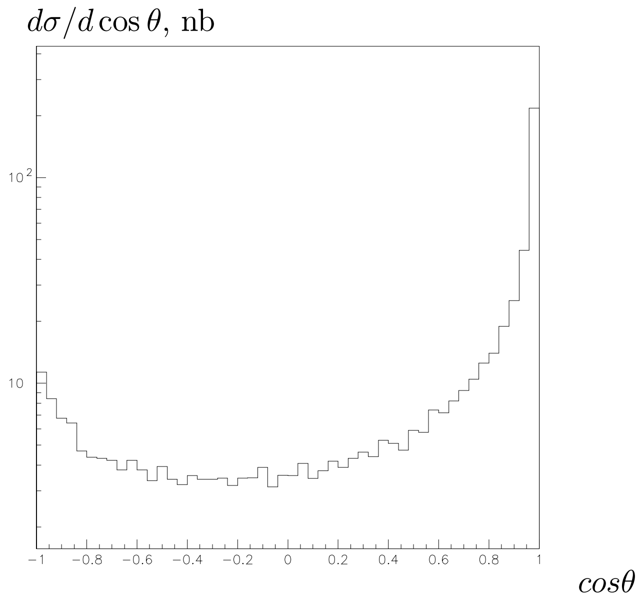

Fig. 4. The $d\sigma/d\cos\theta$ distribution over the angle of θ between the B_c meson and $\bar{c}$-quark in the system of mass centre for the colliding proton beams at the energy of 8 TeV.

Thus, the production of B_c meson is associated with the production of D meson moving in the same direction as B_c, i.e. the D velocity is almost parallel to the B_c one, $\theta < 18^0$. The average transverse momentum of D meson is less than that of B_c (see Fig. 5) in this event . As the detection of B_c meson supposes the observation of secondary vertex, two vertices must be searched for in the same jet in the events with B_c. These are the vertices from the B_c and D meson decays. The correlation between the energy of B_c meson and c-quark associated with it is shown in Fig. 6. A rough estimate shows that the c-quark energy is approximately the same as that of B_c. Taking into account the fact, that after the fragmentation the average D-meson energy equals $\langle E_D \rangle \sim 0.6 \langle E_c \rangle$, and also the average lifetime of B_c is approximately two times less than that of the D^+ meson it is easily to obtain the estimates of the distances between the primary interaction point and the decay vertices of D meson and B_c.

$$x_D \approx \frac{E_c}{M_D}\, 0.6 c\tau_D, \qquad x_{B_c} \approx \frac{E_{B_c}}{M_{B_c}}\, c\tau_{B_c} \ ,$$

i.e.

$$\frac{x_D}{x_{B_c}} \simeq 3.6 \ .$$

Thus, in the events with B_c one should expect also, for example, the associated production of D^+ mesons, having approximately three times greater displacement from the primary vertex of interaction for the particles from the beams, than the displacement of B_c, and the direction of D-meson motion approximately coincides with that of B_c. This configuration can be useful for the extraction of a signal from the hadronic background.

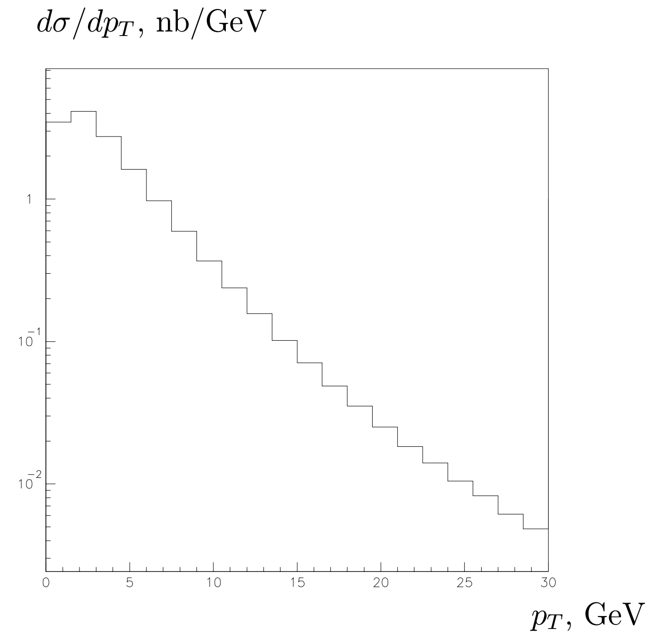

Fig. 5. The distribution over the transverse momentum of the $\bar{c}$-quark associated with the B_c meson in proton-proton interactions at the energy of 8 TeV.

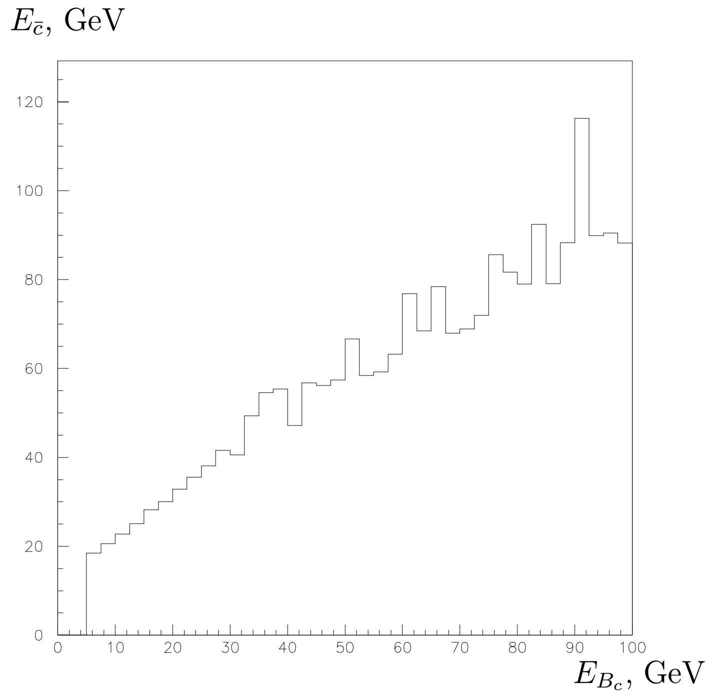

Fig. 6. The correlation between the energies of the B_c meson and $\bar{c}$-quark associated with the former at the LHC energy of 8 TeV.

Conclusion

In this paper we have considered the production mechanism for the different spin S- and P-wave states of the B_c mesons in the hadron interactions at the LHC energies on the basis of calculation for the complete set of diagrams for the leading $O(\alpha_s^4)$-contribution of the perturbative QCD for the hard production of heavy quarks and in the potential model of soft binding of the $\bar{b}$ and c quarks into the meson. One has found that the regime of $\bar{b}$-quark fragmentation into the B_c meson is delayed to the region of large transverse momenta, $p_T > 6M_{B_c} \gg M_{B_c}$, so that the diagrams of the nonfragmentational type, i.e. the recombinations, give the dominant contribution into the total cross-section for the hadronic production of B_c. At the maximum luminosity $\mathcal{L} = 10^{34}$ cm^{-2}c^{-1}, being planned, one should expect the yield of B_c at the level of $3 \cdot 10^{10}$ events per year at $\sqrt{s} = 8$ TeV and $6 \cdot 10^{10}$ events per year at $\sqrt{s} = 16$ TeV.

The theoretical predictions of spectroscopic characteristics for the B_c-meson family and their decays allow one to carry out an object-oriented search for the events with B_c and to extract them from the hadron background. For example, in the semileptonic decay mode of $B_c^+ \to \psi l^+ \nu_l$ with the account of the branching ratio for the leptonic decay of $\psi \to l^+ l^-$ and the efficiency of the detection for the secondary vertex with three leptons $\epsilon = 0.1$, one should expect $12 \cdot 10^6$ reconstructed events with the B_c mesons at $\sqrt{s} = 16$ TeV. Even in the regime of low energies ($\sqrt{s} = 8$ TeV) and luminosity ($\mathcal{L} = 10^{32}$ cm^{-2}c^{-1}) it is possible to reconstruct $6 \cdot 10^4$ semileptonic B_c decays only in the muon channel, for example. The probability of the $B_c^+ \to \psi\pi^+$ decay has the uncertainty related with the large momentum of the recoil ψ meson. In the regime of low energies and luminosity the number of the reliably detected events is about $(0.4-4)\cdot 10^4$ at the same efficiency of detection of the secondary vertex ($\epsilon = 0.1$). It is worth mentioning that we have pointed out the number of events with no account for the detector cuts off the angles and momenta in conditions of particular facilities at LHC. Nevertheless, the search for B_c at LHC seems to be the most promising for a positive result, since, for example, at the LEP facilities the observation of B_c is extremely problematic due to the low yield of B_c. At HERA-B a strong threshold effect for the hadron production of B_c will appear because one has to produce an additional pair of heavy B and D mesons in the final state. So, the statistics at HERA-B will be at the same level as that of LEP, and, in addition, it will have conditions of a more intensive hadron background. A low ratio of the signal to a background also does not yet allow the CDF collaboration (FNAL) to observe the events with B_c because of a low efficiency of the reconstruction for the secondary vertex [32].

Thus, the search for the B_c meson at LHC thinks to be a quite interesting and solvable problem.

This work is in part supported by Russian Foundation for Basic Research, grant 96-02-18216.

References

[1] S.S.Gershtein et al., Uspekhi Fiz. Nauk 165, 3 (1995).

[2] S.S.Gershtein et al., Phys. Rev. D51, 3613 (1995).

[3] E.Eichten, C.Quigg, Phys. Rev. D49, 5845 (1994).

[4] V.V.Kiselev, Mod. Phys. Lett. A10, 1049 (1995);
V.V.Kiselev, Int. J. Mod. Phys. A9, 4987 (1994);
V.V.Kiselev, A.K.Likhoded, A.V.Tkabladze, Yad. Fiz. 56, 128 (1993);
V.V.Kiselev, A.V.Tkabladze, Yad. Fiz. 48, 536 (1988);
G.R.Jibuti, Sh.M.Esakia, Yad. Fiz. 50, 1065 (1989), Yad. Fiz. 51, 1681 (1990);
C.-H.Chang, Y.-Q.Chen, Phys. Rev. D49, 3399 (1994).

[5] M.Lusignoli, M.Masetti, Z. Phys. C51, 549 (1991).

[6] M.Beneke, G.Buchalla, Phys. Rev. D53, 4991 (1996);
I.Bigi, Phys. Lett. B371, 105 (1996).

[7] L.Clavelli, Phys. Rev. D26, 1610 (1982);
C.-R.Ji and R.Amiri, Phys. Rev. D35, 3318 (1987);
C.-H.Chang and Y.-Q.Chen, Phys. Lett. B284, 127 (1992).

[8] C.-H.Chang, Y.-Q.Chen, Phys. Rev. D46, 3845 (1992), D50, 6013(E) (1994);
E.Braaten, K.Cheung, T.C.Yuan, Phys. Rev. D48, 4230 (1993);
V.V.Kiselev, A.K.Likhoded, M.V.Shevlyagin, Z. Phys. C63, 77 (1994);
T.C.Yuan, Phys. Rev. D50, 5664 (1994);
K.Cheung, T.C.Yuan, Phys. Rev. D53, 3591 (1996).

[9] A.V.Berezhnoy, A.K.Likhoded, M.V.Shevlyagin, Phys. Lett. B342, 351 (1995);
K.Kolodziej, A.Leike, R.Rückl, Phys. Lett. B348, 219 (1995);
A.V.Berezhnoy, V.V.Kiselev, A.K.Likhoded, Phys. Lett. B381, 341 (1996).

[10] A.V. Berezhnoy, A.K. Likhoded, M.V. Shevlyagin, Yad. Fiz. 58, 730 (1995);
A.V. Berezhnoy, A.K. Likhoded, O.P. Yuschenko, Yad. Fiz. 59, 742 (1996);
C.-H.Chang et al., Phys. Lett. B364, 78 (1995);
K. Kolodziej, A.Leike, R.Rückl, Phys. Lett. B355, 337 (1995);
A.V.Berezhnoy, V.V.Kiselev, A.K.Likhoded, Z. Phys. A356, 79 (1996).

[11] C.Quigg, J.L.Rosner, Phys. Rep. 56, 167 (1979).

[12] M.A.Shifman, A.I.Vainshtein, V.I.Zakharov, Nucl. Phys. B147, 385, 448 (1979);
L.J.Reinders, H.Rubinstein, T.Yazaki, Phys. Rep. 127, 1 (1985).

[13] G.T.Bodwin, E.Braaten, G.P.Lepage, Phys. Rev. D51,1125 (1995);
T.Mannel, G.A.Schuller, Z. Phys. C67, 159 (1995).

[14] R.M.Barnett et al., PDG, Phys. Rev. D54, 1 (1996).

[15] E.Eichten, Preprint FERMILAB-Conf-85/29-T (1985).

[16] C.Quigg, J.L.Rosner, Phys. Lett. B71, 153 (1977).

[17] A.Martin, Phys. Lett. B93, 338 (1980).

[18] E.Eichten, F.Feinberg, Phys. Rev. Lett. 43, 1205 (1979), Phys. Rev. D2, 2724 (1981);
D.Gromes, Z. Phys. C26, 401 (1984).

[19] W.Buchmüller, S.-H.H.Tye, Phys. Rev. D24, 132 (1981).

[20] E.Braaten, S.Fleming, Phys. Rev. D52, 181 (1995).

[21] V.V.Kiselev, Int. J. Mod. Phys. A11, 3689 (1996); Nucl. Phys. B406, 340 (1993).

[22] M.B.Voloshin, Int J. Mod. Phys. A10, 2865 (1995).

[23] V.V.Kiselev, Mod. Phys. Lett. A10, 2113 (1995); Preprint IHEP 96-63 (1996) [hep-ph/9608435] to appear in Phys. Lett. B.

[24] M.Neubert, Phys. Rep. 245, 259 (1994).

[25] V.V.Kiselev, Phys. Lett. B362, 173 (1995).

[26] P.Colangelo, G.Nardulli, N.Paver, Z. Phys. C57, 43 (1993);
E.Bagan at al., Z. Phys. C64, 57 (1994).

[27] V.V.Kiselev, A.V.Tkabladze, Phys. Rev. D48, 5208 (1993).

[28] M.Dugan and B.Grinstein, Phys. Lett. B255, 583 (1991);
M.A.Shifman, Nucl. Phys. B388, 346 (1992);
B.Blok, M.Shifman, Nucl. Phys. B389, 534 (1993).

[29] V.V.Kiselev, Phys. Lett. B372, 326 (1996), Preprint IHEP 96-41 (1996) [hep-ph/9605451].

[30] G.Alexander et al., OPAL Coll., Z. Phys. C70, 197 (1996);
M.L.Andrieux et al., DELPHI Coll., Report pa01-050 at ICHEP'96, Warsaw (1996);
ALEPH Coll., Report pa01-069 at ICHEP'96, Warsaw (1996).

[31] H.L.Lai et al., CTEQ Coll., Preprint MSUHEP-60426 (19960 [hep-ph/9606399].

[32] F.Abe et al., CDF Coll., FERMILAB-Conf-95/202-E (1995).

Received January 14, 1997

А.В.Бережной и др.
B_c-мезон на LHC.

Оригинал-макет подготовлен с помощью системы LaTeX.
Редактор Е.Н.Горина. Технический редактор Н.В.Орлова.

Подписано к печати 14.01.97. Формат $60 \times 84/8$. Офсетная печать.
Печ.л. 2,62. Уч.-изд.л. 2,01. Тираж 250. Заказ 958. Индекс 3649.
ЛР №020498 17.04.97.

ГНЦ РФ Институт физики высоких энергий
142284, Протвино Московской обл.

Индекс 3649

П Р Е П Р И Н Т 97-2, И Ф В Э, 1997